Intercontinental Geoinformation Days

http://igd.mersin.edu.tr/2020/

Using Interquartile Range to Detect TEC Perturbations Associated with A Tropical Cyclone Crossing through The South China Sea

Mohamed Freeshah [*1,4,5], **Xiaohong Zhang** [2,3,4], **Xiaodong Ren** [2]

[1] *Wuhan University, State Key Laboratory of Information Engineering in Surveying, Mapping and Remote Sensing, Wuhan 430079, China*
[2] *Wuhan University, School of Geodesy and Geomatics, Wuhan 430079, China*
[3] *Key Laboratory of Geospace Environment and Geodesy, Ministry of Education, 129 Luoyu Road, Wuhan 430079, China*
[4] *Collaborative Innovation Center for Geospatial Technology, 129 Luoyu Road, Wuhan 430079, China*
[5] *Benha University, Faculty of Engineering at Shoubra, Surveying Engineering Department, Cairo, Egypt*

Keywords
GNSS
Ionosphere
Mangkhut
Interquartile Range
Total electron content

ABSTRACT

In this paper, we investigate the highest amplitude ionospheric variations, maximum sustained wind speed, and typhoon cloud during an extremely powerful tropical cyclone (TC) crossing through the South China Sea in September 2018 that caused extensive damage in Guam, the Philippines, and South China. Regional Ionosphere Maps (RIMs) were created through Hong Kong SatRef and IGS data around the Mangkhut Typhoon. RIMs are utilized to analyze the ionospheric response over the maximum wind speed points (maximum spots) after taking the solar-terrestrial environment and geomagnetic storm indices into consideration. The total electron content (TEC) time sequences over the maximum spots are detected by the method of interquartile range method (IQR) during super typhoon Mangkhut. The research findings indicating that significant ionospheric variations are detected over the maximum spots during the powerful typhoon within a few hours before the extreme wind speed. All the ionospheric variations are positive values. The infrared satellite snapshots confirmed that the maximum ionospheric perturbations do not coincide with the center of the storm but are detected in the area close to the typhoon edges. The possible ionospheric response mechanism is based on strong convective cells which create the gravity waves over TCs.

1. INTRODUCTION

Solar radiation and geomagnetic storms play a crucial role in the dynamic regime of the ionosphere (Sojka et al, 1981). However, some ionospheric perturbations should be interpreted by tropospheric activities (Chane-ming et al., 2002); (Guha et al., 2016). In 1960, the theoretical studies of atmospheric acoustic gravity waves (AGWs) have been indicated that the ionosphere could respond to severe weather activities for instance lightning, cyclones, tornadoes, and hurricanes (Hine, 1960).

For the first time, (Bauer, 1958) has reported the findings of the ionospheric response to typhoon passage where the F2 layer's critical frequency was increased when the typhoon getting close to the High-Frequency (HF) Radio station. The electric field and ion oscillation in a studied region would enhance according to the strength of the cyclone, and this depends on charged aerosols and droplets (Isaev et al., 2010, 2002). On the same side, (Sorokin et al., 2005; Pulinets et al., 2000) have reinforced that an ionospheric plasma irregularity may be generated over the regions of powerful synoptic perturbations for the electric fields.

Recently, the Global Navigation Satellite System (GNSS) has a fast development and the number of GNSS receivers has been increased globally and domestically. The ionospheric response to typhoon could be studied by using GNSS sounding and calculating the total electron content (TEC) through ground GNSS station. Although the highest amplitudes of TEC variation have been recorded during the cyclone's maximum wind speed (maximum spot) (Polyakova and Perevalova, 2013). Many previous studies have been concentrated more on ionospheric variations associated with TCs on the day of typhoon landfall (Guha et al., 2016; Jun Chen et al., 2020; Song et al., 2019). W. Li et al., 2017 have used the TEC

* **Corresponding Author**

*(mohamedfreeshah@whu.edu.cn) ORCID ID 0000-0003-3539-7450
(xhzhang@sgg.whu.edu.cn) ORCID ID xxxx-xxxx-xxxx-xxxx
(renxiaodongfly@gmail.com) ORCID ID xxxx-xxxx-xxxx-xxxx

Cite this study

Freeshah M, Zhang X and Ren X (2020). Using Interquartile Range to Detect TEC Perturbations Associated with A Tropical Cyclone Crossing through The South China Sea. Intercontinental Geoinformation Days (IGD), 28-31, Mersin, Turkey

maps from the Center for Orbit Determination in Europe (CODE) to detect the ionospheric disturbances during the passing of powerful TC's. The produced TEC maps from CODE have a limited spatial resolution of 2.5 degrees in latitude versus 5 degrees in longitude, moreover, it depends mainly on IGS stations.

In this study, we produced the ionosphere maps with a spatial grid 0.2*0.4 degree in latitude and longitude, respectively, with 2 hrs as a temporal resolution by using dense CORS in Hong Kong and IGS stations around the typhoon. Besides, the interquartile range method was used for checking possible TEC disturbances over maximum spots.

2. DATA AND METHODS

2.1. Space and Mangkhut data

We collected the GNSS observations from IGS and the Hong Kong Satellite Positioning Reference Station Network (SatRef) in the area around the typhoon. the F10.7 cm is an indicator of solar activity, the Disturbance storm-time (Dst), and Kp indices were obtained from NASA OmniWeb Data Explorer. The infrared (IR) satellite snapshots of typhoon Mangkhut's cloud system were selected for certain moments from the Cooperative Institute for the Meteorological Satellite Studies / University of Wisconsin-Madison.

2.2. Calculation of STEC, VTEC, and RIMs

We derived the Slant TEC (STEC) along the line of sight from GNSS constellation satellites to GNSS receivers through Carrier-to-Code Leveling (CCL) method for more details we can refer to (Freeshah et al., 2020; Z. Li et al., 2014). We can express the ionospheric delay in length unit and TEC as a function in ƒ frequency (f1 = 1575.42 MHz, f2 =1227.60 MHz) through the next equation:

$$TEC = \frac{I.f^2}{40.31 \times 10^{16}} \quad (1)$$

where I is the ionospheric delay along a specific line of sight (LOS). According to the modeling-hypothesis of a single shell layer where the 2D modeling process assumes that the total free electrons of the whole ionosphere are concentrated in a thin layer at the elevation with the max electron density (Sidorenko and Vasenina, 2016). The slant TEC value along the LOS at the Ionospheric Pierce Point (IPP) can be converted into the corresponding vertical TEC (VTEC) by using a common ionospheric mapping-function (MF).

$$VTEC = cos\ cos\left[arcsin\ arcsin\left(\frac{R}{R+H} sinz\right)\right] STEC \quad (2)$$

where R represents the average radius of the earth, H denotes the altitude of the ionospheric shell layer, z stands for the satellite zenith angle at the receiver. A dot should be placed after the figure number. We have created a high resolution regional ionospheric maps (RIMs) of 0.2*0.4 degree in latitude and longitude, respectively, around the area of typhoon by the Spherical Harmonics expansion.

To reduce the multipath effect error, the elevation cutoff angle was set to be 15 degrees, besides, the term of windup has been adjusted by orbital information and coordinates of each station.

To discover the possible anomalous signals of the TEC variations, the TEC sequences of 10 days before 11st of September 2018 where the tropical cyclone was classified as Super Typhoon according to HKO, was used as window length to calculate the upper quartile, lower quartile, and median, denoted as QU, QL, and M, respectively, for more details we can refer to (W. Li et al., 2017). During the process of data analysis, the values of TECs over the two maximum spots at the same time are extracted from the RIMs.

The TECs have values outside corresponding to upper or lower boundaries are regarded as abnormal signals where it can be positive or negative anomalies, respectively. The TEC anomalies can last for six hours at least (W. Li et al., 2017). The TEC time series were analyzed for the next seven days (from Doy254-Doy260) during Super Typhoon Mangkhut over the two maximum spots.

3. RESULTS

According to the recorded data for the Maximum sustained-wind near the center of the Mangkhut, there are two points with maximum wind speed at all. Figure 1 shows the maximum wind speed is 250 km/hr over the positions (17.7 N, 123.2 E) at 23:00 HKT on 14 September 2018 and (18.0 N, 122.3 E) at 02:00 HKT on 15 September 2018.

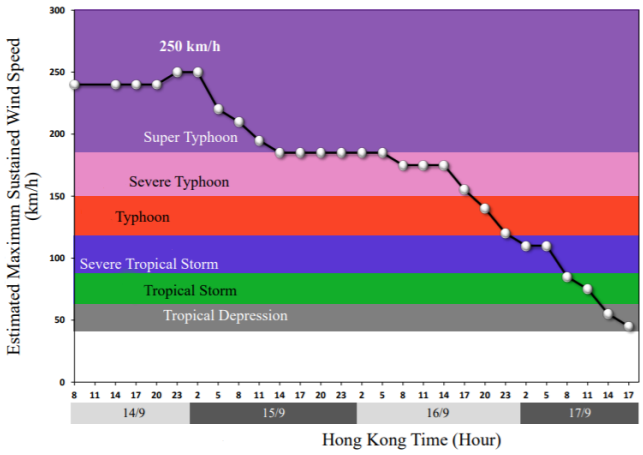

Figure 1. Air intensity from Sep 14th -17th with colors representing the typhoon classification

To distinguish whether the space weather impacts on TEC deviations during the typhoon, the F10.7, the Disturbance storm-time (Dst), and geomagnetic Kp indices have been investigated before analyze TEC variations associated with typhoons. Figure 2 shows no existence of a strong solar activity or geomagnetic activity. There is a low geomagnetic activity (Kp≤4), except on the Doy257 Kp≤4.3, Doy253 Kp≤5, and the Doy254 that has the highest value of Kp ≤ 6, indicating a moderate geomagnetic activity, Doy254 was excluded from the IQR window length to skip the variation based on geomagnetic activity.

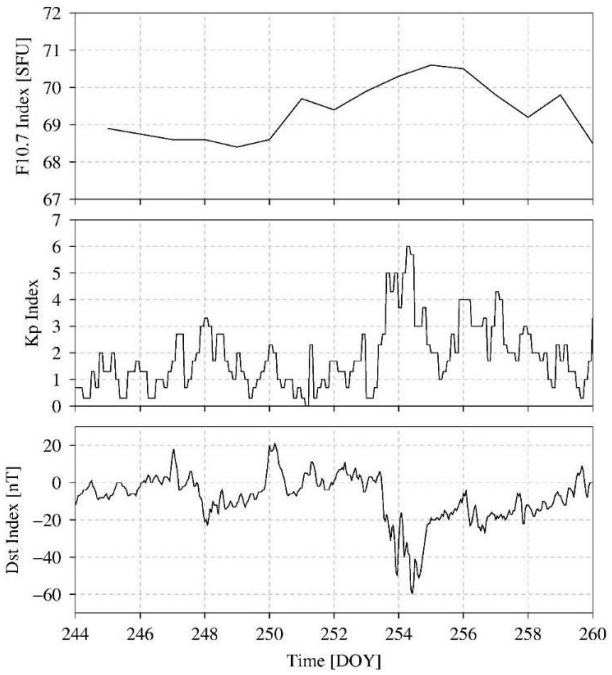

Figure 2. F10.7, Kp, and Dst indices in the period from DOY 244 to DOY 260 of 2018

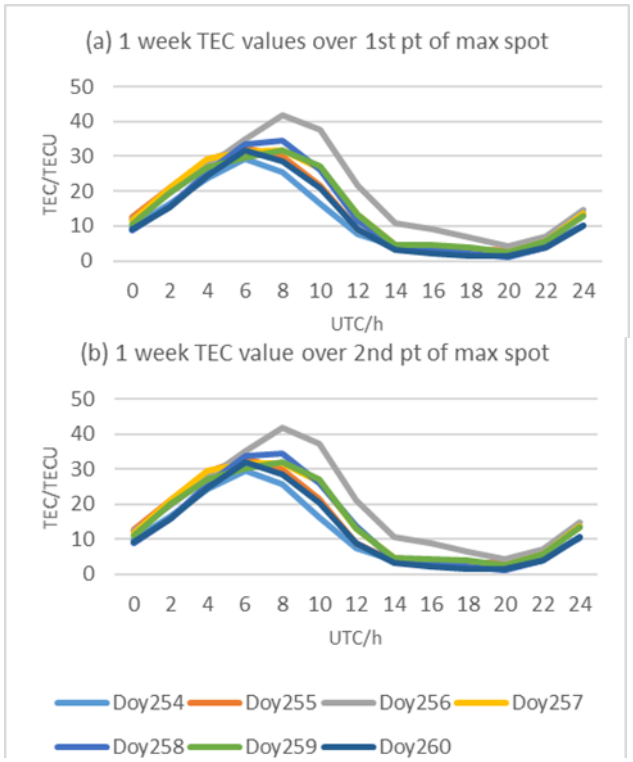

Figure 3. (a) and (b) TEC values over 1st and 2nd maximum spots of the Mangkhut, from Sep 11 to Sep 17

Figure 3 shows the TEC time series values for 24 hrs/week over the 1st and 2nd max spots during the typhoon. The range of 34.55-1.2 TECU was maintained for most of the time during the typhoon except for Doy256 where the range increased significantly to become 41.9-4.2 TECU, Figure 3(a). For Doy256, TEC gradually increased to the maximum value of about 8 am UT, then TEC gradually decreased. As shown in Figure 3(b), the range of 34.6-1.25 TECU was maintained for most of the time during the typhoon except for Doy256 where the range increased significantly to become 42.05-4.35 TECU. For Doy256, TEC gradually increased to the maximum value of about 8 am UT, then TEC gradually decreased.

To verify the previous TEC variations on Doy 256, parameters of interquartile range method UQ, MQ, LQ, and IQR were calculated from the 10 days before the Mangkhut typhoon (from Doy244-Doy253). l1 and l2 can be calculated by taking twice the IQR as a tolerance (~2.7 standard deviations), where l1 and l2 are the lower and upper boundaries, respectively. Figure. 4 shows the TEC time series of Doy256 in gray color versus the lower and upper boundaries in blue and orange colors, respectively. Figure. 4(a) and (b) show significantly increased in TEC over the 2 maximum wind speed points last about 6–14 UT. The lower and upper boundaries used to discriminate the ionospheric anomalies response to typhoon depend on the IQR through the 10 previous days before the cyclone converted into a super typhoon. It is worth indicating that the ionospheric disturbances showed in Figure 4 is a positive value and agree with the general behavior in Figure 3.

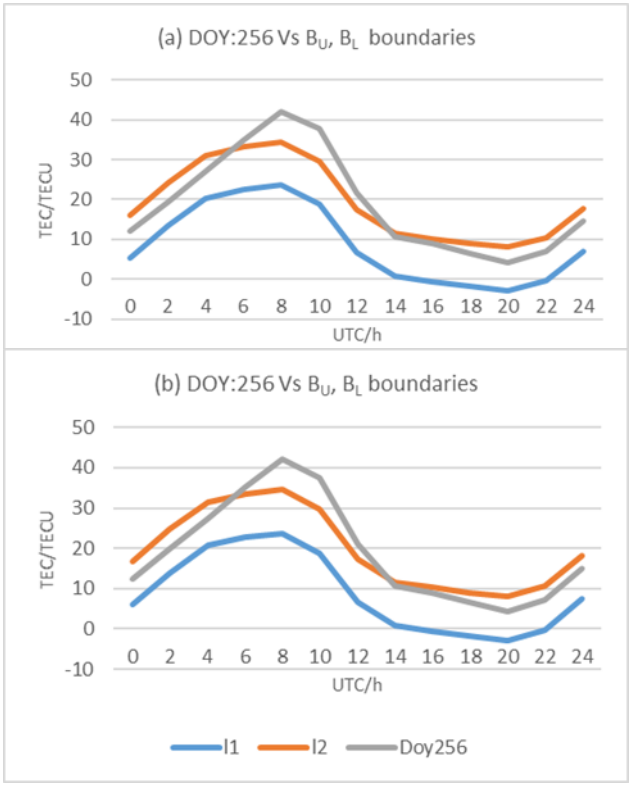

Figure 4. (a) and (b) TEC lower and upper boundaries (l1 and l2, respectively) of the IQR method versus the TEC sequences of Doy256

4. DISCUSSION

(Polyakova and Perevalova, 2013; W. Li et al., 2017) have shown that during the day of the maximum wind speed value over the TC, the highest amplitude of TEC variation was observed. In contrast, the current study showing that the highest TEC variation amplitude was observed on September 13 (Doy256) when the wind speed in the TC had a second-highest value. To interpret the possible reasons, the infrared satellite snapshots of typhoon cloud at 4 selected time instances are depicted in Figure 5. The red triangle shows the maximum spots.

The panels (a) to (d) show the position and tracking of the Typhoon direction from southeast to northwest and ended on 16th September (panel (d)). Panel (b) shows an instance on 13th September where the maximum spot is far away from the typhoon's center (eye) and more close to the edge of the typhoon, meanwhile, panel (c) shows the maximum spot close to the typhoon's eye on September 14 (the day of maximum wind speed), that could explain why the highest TEC variations have happened in the second-highest wind speed where the magnitude of the ionospheric perturbation is depending on the distance away/close from the typhoon (Jun Chen et al., 2020). This implies that ionospheric perturbations in the eye of the storm are fewer than those at the edges of cyclones (W. Li et al., 2017).

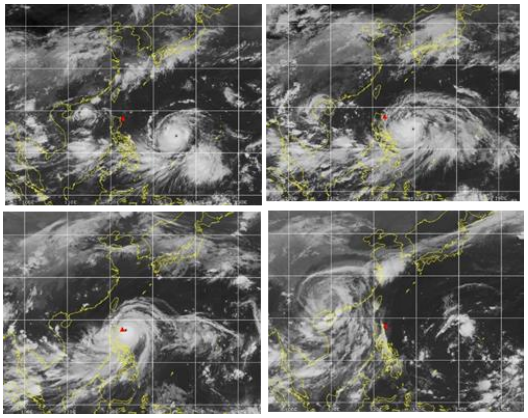

Figure 5. IR satellite snapshots of typhoon cloud at 4-time instances, the red triangle denotes maximum spots, (a): 04:30/12 (UTC); (b) 07:30/13; (c) m, (d) 22:30/16

REFERENCES

Bauer, S. J. (1958). Correlations between tropospheric and ionospheric parameters. Geofisica Pura e Applicata, 40, 235–240. https://doi.org/https://doi.org/10.1007/BF0198131

Chane-ming, F., Roff, G., Robert, L., & Leveau, J. (2002). Gravity wave characteristics over Tromelin Island during the passage of cyclone Hudah. Geophysical Research Letters, 29(6). https://doi.org/http://dx.doi.org/10.1029/2001G013286

Freeshah, M., Zhang, X., Chen, J., Zhao, Z., Osama, N., Sadek, M., & Twumasi, N. (2020). Detecting Ionospheric TEC Disturbances by Three Methods of Detrending through Dense CORS During A Strong Thunderstorm. Annals of Geophysics. In Press

Guha, A., Paul, B., Chakraborty, M., & De, B. K. (2016). Tropical cyclone effects on the equatorial ionosphere: First result from the Indian sector. Journal of Geophysical Research: Space Physics, 121, 5764–5777. https://doi.org/10.1002/2016JA022363.

Hine, C. O. (1960). Internal atmospheric gravity waves at ionospheric heights. Canadian Journal of Physics, 38(11).

Jun Chen, Xiaohong Zhang, Xiaodong Ren, Jincheng Zhang, Mohamed Freeshah, & Zhibo Zhao. (2020). Ionospheric disturbances detected during a typhoon based on GNSS phase observations: A case study for typhoon Mangkhut over Hong Kong. Advances in Space Research, In press. https://doi.org/https://doi.org/10.1016/j.asr.2020.06.006

Li, W., Yue, J., Yang, Y., Li, Z., Guo, J., Pan, Y., & Zhang, K. (2017). Analysis of ionospheric disturbances associated with powerful cyclones in East Asia and North America. Journal of Atmospheric and SolarTerrestrial Physics, 161(June), 43–54. https://doi.org/10.1016/j.jastp.2017.06.012

Li, Z., Yuan, Y., Fan, L., Huo, X., & Hsu, H. (2014). Determination of the Differential Code Bias for Current BDS Satellites. IEEE Transactions on Geoscience and Remote Sensing, 52(7), 3968–3979. https://doi.org/10.1109/TGRS.2013.2278545

N. V. Isaev, V. M. Kostin, G. G. Belyaev, O. Ya. Ovcharenko, & E. P. Trushkina. (2010). Disturbances of the topside ionosphere caused by typhoons. Geomagnetism and Aeronomy, 50, 243–255. https://doi.org/https://doi.org/10.1134/S001679321002012X

N. V. Isaev, V. M. Sorokin, V. M. Chmyrev, O. N. Serebryakova, & A. K. Yashchenko. (2002). Disturbance of the Electric Field in the Ionosphere by Sea Storms and Typhoons. Geomagnetism and Aeronomy, 40(5), 638–643.

Polyakova, A. S., & Perevalova, N. P. (2013). Comparative analysis of TEC disturbances over tropical cyclone zones in the North-West Pacific Ocean. Advances in Space Research, 52(2013), 1416–1426. https://doi.org/10.1016/j.asr.2013.07.029

S. A. Pulinets, K. A. Boyarchuk, V. V. Hegai, V. P. Kim, & A. M. Lomonosov. (2000). Quasielectrostatic model of atmosphere-thermosphere-ionosphere. Advances in Space Research, 26(8), 1209–1218.https://doi.org/https://doi.org/10.10-16/S0273-1177(99)01223-5

Sidorenko, K. A., & Vasenina, A. A. (2016). Ionospheric parameters estimation using GLONASS / GPS data. Advances in Space Research, 57, 1881–1888. https://doi.org/10.1016/j.asr.2016.01.025

Sojka, J. J., Raitt, W. J., & Schunk, R. W. (1981). Theoretical predictions for ion composition in the high-latitude winter F-region for solar minimum and low magnetic activity. J. Geophys. Res., 86, 2206– 2216. https://doi.org/https://doi.org/10.1029/JA086iA04p02206

Song, Q., Ding, F., Zhang, X., Liu, H., Mao, T., Zhao, X., & Wang, Y. (2019). Medium-Scale Traveling Ionospheric Disturbances Induced by Typhoon Chan-hom Over China. Journal of Geophysical Research: Space Physics, 124(3), 2223–2237. https://doi.org/10.1029/2018JA026152

Sorokin, V. M., Isaev, N. V, Yaschenko, A. K., Chmyrev, V. M., & Hayakawa, M. (2005). Strong DC electric field formation in the low latitude ionosphere over typhoons. Atmospheric and Solar-Terrestrial Physics, 67(2005), 1269–1279. https://doi.org/10.1016/j.jastp.2005.06.014